Coordinated transport of phosphorylated amyloid-β precursor protein and c-Jun NH_2-terminal kinase–interacting protein-1

Zoia Muresan and Virgil Muresan

Department of Physiology and Biophysics, Case School of Medicine, Case Western Reserve University, Cleveland, OH 44106

The transmembrane protein amyloid-β precursor protein (APP) and the vesicle-associated protein c-Jun NH_2-terminal kinase–interacting protein-1 (JIP-1) are transported into axons by kinesin-1. Both proteins may bind to kinesin-1 directly and can be transported separately. Because JIP-1 and APP can interact, kinesin-1 may recruit them as a complex, enabling their cotransport. In this study, we tested whether APP and JIP-1 are transported together or separately on different vesicles. We found that, within the cellular context, JIP-1 preferentially interacts with Thr^{668}-phosphorylated APP (pAPP), compared with nonphosphorylated APP. In neurons, JIP-1 colocalizes with vesicles containing pAPP and is excluded from those containing nonphosphorylated APP. The accumulation of JIP-1 and pAPP in neurites requires kinesin-1, and the expression of a phosphomimetic APP mutant increases JIP-1 transport. Down-regulation of JIP-1 by small interfering RNA specifically impairs transport of pAPP, with no effect on the trafficking of nonphosphorylated APP. These results indicate that the phosphorylation of APP regulates the formation of a pAPP–JIP-1 complex that accumulates in neurites independent of nonphosphorylated APP.

Introduction

In neurons, membrane-bound cargoes are transported into axons by kinesin motors such as kinesin-1 (Muresan, 2000). Because the rate of the delivery of proteins into axons should meet the needs of the individual proteins at the destination, the formation of the transport vesicle and recruitment of the required kinesin motor have to be highly regulated. This study addresses the regulation of the axonal transport of two kinesin-1 cargoes, the amyloid-β precursor protein (APP) and the c-Jun NH_2-terminal kinase (JNK)–interacting protein-1 (JIP-1).

Kinesin-1 is recruited to its vesicular cargoes by transmembrane or cytoplasmic vesicle–associated proteins that interact with either the kinesin light chain (KLC) or kinesin heavy chain (KHC). Among the proposed kinesin-1 cargo linkers are APP and JIP-1. APP, the precursor of the amyloid-β peptide that forms the senile plaques in Alzheimer's disease, is a type-I transmembrane protein (Selkoe, 1998), whereas JIP-1 is a scaffolding protein for the JNK signaling complex that, although not an integral membrane protein, is associated with intracellular membranes (Whitmarsh et al., 1998). APP and JIP-1 have been reported to interact with the tetratricopeptide repeat (TPR) domain of KLC (Kamal et al., 2000; Whitmarsh et al., 2001; Verhey et al., 2001), suggesting that each of them can be transported by kinesin-1 as an independent cargo. JIP-1 can also bind to APP via its phosphotyrosine-binding domain and the YENPTY-containing site in the cytoplasmic tail of APP (Matsuda et al., 2001; Scheinfeld et al., 2002; Taru et al., 2002). Upon exogenous expression, this complex recruits expressed KLC, suggesting the possibility of the cotransport of APP bound to JIP-1 (Inomata et al., 2003). Whether in normal conditions APP and JIP-1 are transported as a complex or independently is not known, and is certainly determined by the type of interactions that the endogenous proteins establish both between themselves and with kinesin-1.

Starting from the premise that the in vivo interaction of APP with JIP-1 has to be regulated, we tested whether the phosphorylation of residues in the cytoplasmic domain of APP plays any role in the formation of the APP–JIP-1 complex. Recent studies have focused on the phosphorylation of Thr^{668} (human APP695 isoform numbering), which has been implicated in neuronal differentiation (Ando et al., 1999), APP processing (Lee et al., 2003), and the accumulation of an APP cytoplasmic

Correspondence to Zoia Muresan: zoia.muresan@case.edu; or Virgil Muresan: virgil.muresan@case.edu

Abbreviations used in this paper: APP, amyloid-β precursor protein; JIP-1, JNK-interacting protein-1; JNK, c-Jun NH_2-terminal kinase; KHC, kinesin heavy chain; KLC, kinesin light chain; pAPP, Thr^{668}-phosphorylated APP; PP5, protein phosphatase 5; siRNA, small interfering RNA; TPR, tetratricopeptide repeat.

The online version of this article contains supplemental material.

The Journal of Cell Biology, Vol. 171, No. 4, November 21, 2005 615–625
http://www.jcb.org/cgi/doi/10.1083/jcb.200502043

fragment in the nucleus (Muresan and Muresan, 2004). Thr^{668}-phosphorylated APP (pAPP) is concentrated at neurite endings (Ando et al., 1999; Muresan and Muresan, 2005), suggesting that phosphorylation might also target pAPP into neurites.

Using the catecholaminergic, central nervous system–derived neuronal cell line CAD, we investigated whether APP and JIP-1 are transported on the same carrier vesicle or independently, on distinct vesicles. We focused on studying the transport of endogenous proteins under physiological conditions, an experimental approach intended to avoid the many pitfalls of exogenous protein expression. We found that JIP-1 preferentially interacts with pAPP and is cotransported with pAPP into neuronal processes by kinesin-1. We also discovered that nonphosphorylated APP is transported independently of pAPP and JIP-1. These findings point to a role for APP phosphorylation in the transport of JIP-1, and possibly in regulating signaling cascades assembled on this scaffolding protein.

Results

JIP-1 and APP reside on distinct vesicles throughout neuronal processes

JIP-1 and APP are cargoes for kinesin-1 that could theoretically be transported into neuronal processes, either independently or as a complex. To test the interdependence of transport of endogenous JIP-1 and APP, we set out to determine if these two proteins localize on separate carrier vesicles along the neuronal processes, where most vesicles move anterogradely en route to the neurite terminals, or on the same carrier vesicle (Fig. S1, available at http://www.jcb.org/cgi/content/full/jcb.200502043/DC1; Kaether et al., 2000; Stamer et al., 2002; unpublished data). To this end, we performed high resolution, double labeling immunocytochemistry for JIP-1 and APP in the CAD neuronal cell line.

The specificity of the antibodies used for the immunolocalization of JIP-1 and APP was verified by Western blots of rat brain lysate. Antibodies to JIP-1 detected two polypeptides (Fig. S2 A, available at http://www.jcb.org/cgi/content/full/jcb.200502043/DC1) that correspond to the previously identified forms of endogenous JIP-1 (Meyer et al., 1999). For APP we tested antibodies 22C11 and 4G8, which are frequently used for the detection of total APP (Kamal et al., 2000; Lazarov et al., 2005; Lee et al., 2005). Each of them labeled a band with mobility that was characteristic of APP (Fig. S2 A). However, in this work, we mostly used the antibody 4G8 for immunocytochemistry because 22C11 may cross-react with the amyloid precursor-like protein 2, a protein related to APP (Wasco et al., 1993).

CAD cells have proven suitable for studying the intracellular traffic powered by kinesins (Verhey et al., 2001; Muresan and Muresan, 2005). When cultured in serum-free medium, CAD cells differentiate and gain the biochemical and morphological characteristics of primary neurons in culture (Qi et al., 1997), with thin processes and terminals where transport vesicles and their associated proteins can be resolved using high power fluorescence microscopy. In these cells, transport of APP (see next section) and JIP-1 (Verhey et al., 2001) is kinesin-1 dependent, and the global localization of these proteins (Fig. S2, B and C) is

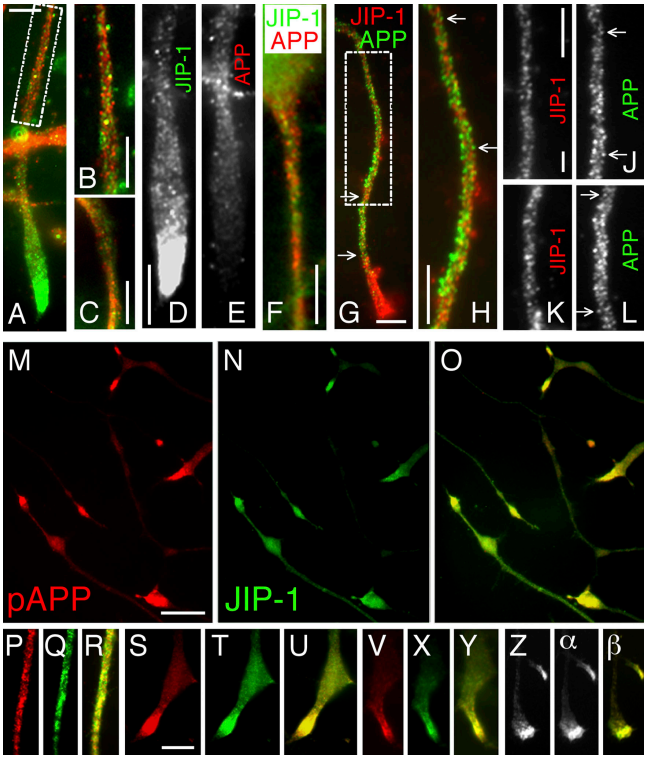

Figure 1. **Colocalization of JIP-1 with pAPP in neuronal processes.** CAD cells (A–F and M–Y) and cortical neurons (G–L, Z–β) were double labeled for JIP-1 and either total APP (antibody 4G8; A–L) or pAPP (M–β). (A–L) The majority of total APP (A–F, red; G–L, green) is present in vesicles distinct from those carrying JIP-1 (A–F, green; G–L, red). (B and H) Enlargements of the boxed areas in A and G. (D and E) Single color enlargements of the process terminal shown in A. Similarly, I–L represent single color enlargements of regions from the distal and proximal neurite shown in G and H to reveal the distinct distribution of JIP-1 and APP along the neurite. (G, H, J, and L) Arrows mark the ends of corresponding segments. (M–β) JIP-1 (M–Y and β, green; α, white) colocalizes extensively with pAPP (M–Y and β, red; Z, white) throughout the processes (P–R) and at their terminals (S–β). Bars: (A–L) 5 μm; (M–O) 20 μm; (P–β) 10 μm.

identical to that in neurons (Yamazaki et al., 1995; Yasuda et al., 1999). We found that JIP-1 immunolabeling (Fig. 1, A–F) is mostly punctuate, suggesting that endogenous JIP-1 is largely associated with vesicles. As previously reported for other neurons (Yasuda et al., 1999), in CAD cells JIP-1 appeared concentrated at the terminals of processes (Fig. S2 B and Fig. 1, A and D). Similar to JIP-1, APP was found in the cell body and processes, in a punctuate appearance typical of vesicle proteins (Fig. 1, A–F). Importantly, the majority of APP (~80%) was not localized to vesicles that contained JIP-1, a result that was consistently obtained using several antibodies to APP and JIP-1. This result was confirmed in primary cultures of cortical neurons that closely reproduce the distribution of these proteins in neurons in situ (Fig. 1, G–L). Based on this set of data, we conclude that only a small fraction of APP is cotransported with JIP-1.

JIP-1 colocalizes and interacts with pAPP rather than with nonphosphorylated APP

We focused on characterizing the fraction of APP that colocalizes with JIP-1. We observed that the accumulation of JIP-1 at

the terminals (Fig. 1, A and G) is strikingly similar to that reported for pAPP (Ando et al., 1999). This raised the question of whether JIP-1 might be carried into processes along with pAPP. To test this hypothesis, we began by studying the distribution of pAPP in CAD cells with an antibody to a phosphorylated polypeptide from a region around pThr^{668} in the cytoplasmic domain of APP. We verified the specificity of this antibody toward pAPP in immunoblots of rat brain extract. A single major band with electrophoretic mobility corresponding to mature APP was detected (Fig. S2 A). In immunocytochemistry, the antibody produced a staining (Fig. S2 D) similar to that reported for pAPP in neurons (Ando et al., 1999; Iijima et al., 2000). This staining was completely abolished by competition with the phosphorylated polypeptide from the cytoplasmic domain of APP (Fig. S2, G and H), but was not affected by the corresponding nonphosphorylated polypeptide (Fig. S2, E and F). These results confirmed the specificity of this antibody for pAPP. Next, we used these antibodies for dual labeling of pAPP and JIP-1 in CAD cells and cortical neurons. As shown in Fig. 1 (M–β), endogenous pAPP colocalized extensively with JIP-1, both at the terminals and throughout the processes. Quantitative measurements of the overlap indicated that ~85% of pAPP colocalized with JIP-1. These results support the notion that JIP-1 and pAPP mostly reside on the same vesicle population, along the neurites and at neurite terminals.

The molecular basis of this result might be the direct interaction between pAPP and JIP-1, which is a known APP-binding protein (Matsuda et al., 2001). Probing for such an interaction in CAD cells proved difficult because of the small amounts of endogenous pAPP and JIP-1. Therefore, we prepared extracts from COS-1 cells transfected with FLAG-tagged JIP-1 and performed in vitro pull-down assays on biotinylated polypeptides comprising the entire cytoplasmic domain of APP, phosphorylated or not, at the residue corresponding to Thr^{668} (Fig. 2, A and B). Polypeptides were collected on streptavidin-Sepharose and analyzed for bound JIP-1 by immunoblotting with antibodies to FLAG. Although JIP-1 interacted with both the phosphorylated and nonphosphorylated forms, at equal amounts of peptides (Fig. 2 B, Ponceau S) it was preferentially captured by the phosphorylated peptide (Fig. 2 B). This result was reproduced by ELISA analysis (Fig. 2 C). In addition, ELISA showed that, at high concentration, JIP-1 binds indiscriminately to the phosphorylated and nonphosphorylated peptides (Fig. 2 C, left). We note that ELISA assays were conducted in the presence of cytosol, using low concentrations of JIP-1–FLAG expressed in HEK 293 cells.

Unlike JIP-1, in the peptide capture assay, JIP-2 bound equally well to the peptides regardless of their state of phosphorylation (Fig. 2 B). Using ELISA, we also confirmed that Fe65, which is an APP-binding protein unrelated to the JIPs, preferentially bound to the nonphosphorylated APP peptide (Fig. 2 C, right; Ando et al., 2001), which validated our ELISA protocol. The interaction between JIP-1 and full-length pAPP was further tested by immunoprecipitation from extracts of CAD cells that expressed ectopic JIP-1–FLAG and human APP695. Under these conditions, a fraction of the expressed APP becomes phosphorylated (Muresan and Muresan, 2005). As shown in Fig. 2 D,

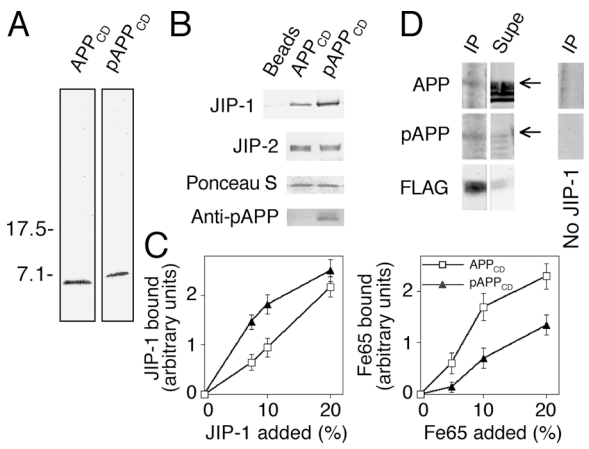

Figure 2. **Biochemical analysis of JIP-1 interaction with nonphosphorylated and phosphorylated APP.** (A) SDS-PAGE separation of synthetic, biotinylated, phosphorylated (pAPP$_{CD}$), and nonphosphorylated (APP$_{CD}$) polypeptides encompassing the APP cytoplasmic domain (Tris-tricine gel). Peptides were detected on the same gel, but the lanes are presented in separate boxes to indicate that the contrast was adjusted differently for each lane. This was done to demonstrate the purity of the peptides rather than their relative amounts. (B) Pull-down experiment done with the polypeptides shown in A. Equal amounts of the two polypeptides (Ponceau S) were incubated with lysates of COS-1 cells transfected with FLAG-tagged JIP-1 or JIP-2 and collected on streptavidin-Sepharose. Copurified JIPs were detected by immunoblotting with antibodies to the FLAG tag (marked JIP-1 and JIP-2). Note that JIP-1, but not JIP-2, binds preferentially to pAPP$_{CD}$. Densitometric analysis of blots showed that JIP-1 binding to APP$_{CD}$ is 30–40% lower than to pAPP$_{CD}$. A control lane (Beads) shows residual binding of JIP-1–FLAG to beads in the absence of added polypeptide. The anti-pAPP antibody detects the phosphorylated, but not the nonphosphorylated, polypeptide in the pulled-down material (Anti-pAPP). (C) Differential binding of JIP-1 and Fe65 to phosphorylated and nonphosphorylated APP polypeptides (ELISA). Streptavidin-coated ELISA plates, preadsorbed with biotinylated APP$_{CD}$ or pAPP$_{CD}$, were incubated with increasing concentrations of cytosol (expressed as percentages of the total incubation mixture; see Materials and methods) from HEK293 cells transfected with either JIP-1–FLAG or Fe65-myc. Bound proteins were detected colorimetrically, using alkaline phosphatase–labeled antibodies to the tags. Error bars represent SEM (n = 3). (D) Coprecipitation of phosphorylated and nonphosphorylated APP with JIP-1. CAD cells were transfected separately with human APP695 and with JIP-1–FLAG; the two cell extracts were mixed and incubated overnight. Mixtures were immunoprecipitated with an anti-FLAG antibody, and immunoprecipitated material was analyzed by immunoblotting with antibodies to total APP, pAPP, and FLAG. The three polypeptides detected with the anti-APP antibody correspond to immature and mature forms of APP695 (arrow points to the fully glycosylated form of APP). (right, No JIP-1) Nonspecific binding of APP and pAPP to beads, in the absence of JIP-1–FLAG-containing cytosol, was low.

only a small fraction of the total mature APP coprecipitated with JIP-1. However, a large proportion of the mature, fully glycosylated form of pAPP bound to JIP-1. This result suggests that JIP-1 preferentially associates with pAPP, and not with its nonphosphorylated form. This binding preference for pAPP at low JIP-1 concentrations, although small, may prevail under in vivo conditions and contribute to the colocalization of JIP-1 with pAPP (Fig. 1). Thus, phosphorylation of APP may facilitate the recruitment of JIP-1 to vesicles.

JIP-1 and pAPP are cotransported by kinesin-1 to neurite terminals

Based on the colocalization and preferential interaction of JIP-1 with pAPP, we propose a model for the transport of these pro-

teins into neuronal processes where JIP-1 mediates recruitment of kinesin-1 to pAPP in the cell body, resulting in the transport of the pAPP–JIP-1 complex to the terminals. The model predicts the following: (1) pAPP and JIP-1 colocalize with kinesin-1 in neurites; (2) transport of pAPP—similar to that of JIP-1—is dependent on kinesin-1; (3) phosphorylation of APP occurs in the cell body, before kinesin-1 recruitment and initiation of transport; (4) recruitment of kinesin-1 to pAPP and transport of pAPP are enhanced by JIP-1; (5) transport of JIP-1 into neurites is enhanced by APP phosphorylation; and (6) down-regulation of JIP-1 expression reduces transport of pAPP into neurites. We tested these suppositions as follows.

First, we tested if, consistent with its transport by a kinesin motor, pAPP colocalizes with microtubules throughout the processes of CAD cells (Fig. S3, A–D, available at http://www.jcb.org/cgi/content/full/jcb.200502043/DC1). Further, pAPP colocalizes with KHC (Fig. S3, H–K) and KLC (Fig. S3, L–N) of kinesin-1, but not with another kinesin (Fig. S3, E–G). In these experiments, the KLCs were detected with the antibody 63-90, which preferentially recognizes the nonphosphorylated, cargo-bound form of KLCs (Pigino et al., 2003). This result is important because it suggests that pAPP is associated with kinesin-1 at the neurite terminals, most likely a consequence of prior active transport toward this destination.

Second, to test whether transport of pAPP requires kinesin-1, we used a dominant-negative construct that specifically uncouples this kinesin from the cargoes that bind to the KLCs (Verhey et al., 2001). When we expressed the tagged, kinesin-1 dominant-negative domain HA-KLC-TPR in CAD cells, transport of pAPP was significantly reduced: $<10\%$ of the transfected cells showed pAPP at their terminals (Fig. 3, A–H). By comparison, $\sim 85\%$ of the cells that overexpressed a TPR domain unrelated to that of KLC (that of protein phosphatase 5 [PP5]) showed unperturbed accumulation of pAPP at their terminals (Fig. 3, I and J). These results support our hypothesis that accumulation of JIP-1 and pAPP at the terminals requires kinesin-1.

Third, a closer examination of the KLC-TPR–expressing cells revealed a buildup of pAPP-containing vesicles in the cell bodies at the emergence of the processes (Fig. 3, A and D, arrowheads). This is consistent with impaired transport of pAPP generated in the cell body. Like pAPP, JIP-1 also accumulated in the cell body of cells transfected with KLC-TPRs (Fig. 3, K and L), indicating that transport of pAPP and JIP-1 are regulated by kinesin-1 in a similar manner. Additional data in support of APP phosphorylation in the cell body is provided by immunocytochemistry experiments showing that pAPP associated with vesicular structures in the Golgi region of CAD cells, whether they were nontransfected (Fig. 3, M and N) or transfected with APP-YFP (Fig. 3, O and P). Together, these observations suggest that an interaction with the KLCs of kinesin-1 is required for the transport of pAPP-containing vesicles from the cell body into processes.

Using a similar experimental strategy, we also confirmed that the delivery of total APP into processes largely relies on kinesin-1 (Yamazaki et al., 1995; Kaether et al., 2000), and probably requires an interaction of the APP-containing cargo with the KLCs (Fig. S4, available at http://www.jcb.org/cgi/content/full/jcb.200502043/DC1).

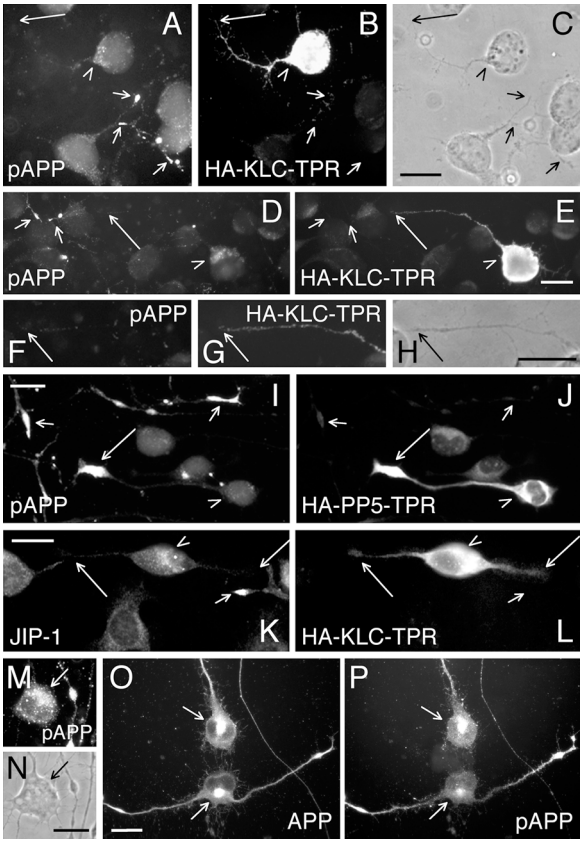

Figure 3. **Localization of pAPP at neurite terminals requires kinesin-1.** (A–L) Localization of pAPP (A–J) and JIP-1 (K and L) in CAD cells overexpressing the tagged, kinesin-1 dominant-negative construct, HA-KLC-TPR (A–H, K, and L), or the control construct, HA-PP5-TPR (I and J). Two examples show the effect of HA-KLC-TPR expression on pAPP localization (A–C and D–H). Note that pAPP and JIP-1 accumulate in the cell body of cells transfected with HA-KLC-TPR (arrowheads) and are not detected at the terminals of their processes (long arrows). In contrast, pAPP and JIP-1 localize to the neurite terminals in nontransfected cells (short arrows). Localization of pAPP is not affected in cells transfected with HA-PP5-TPR (compare short with long arrows in I and J). No pAPP accumulation in the cell body of the transfected cell is seen (I and J, arrowheads). (F–H) Enlarged images of the neurite shown in D and E. (M–P) pAPP can be detected in the Golgi area in CAD cells. (M and N) Vesicular localization of endogenous pAPP in the Golgi region (arrow) of a CAD cell. (O and P) In cells transfected with APP695, pAPP is found throughout the processes and in the cell body (P, arrows). (O) Image depicts total APP. (C, H, and N) Phase-contrast micrographs. Bars, 20 μm.

Fourth, because our model states that JIP-1 and pAPP are transported as a complex, we tested if increased availability of JIP-1 facilitates transport of pAPP to neurite terminals. First, we determined biochemically whether the recruitment of kinesin-1 to pAPP is enhanced by increased amounts of JIP-1. We transfected CAD cells with a mutated human APP695 that mimics pAPP, called APP-Thr668Glu (Ando et al., 1999). Lysates of these cells were mixed with extracts of CAD cells that were JIP-1 transfected or nontransfected (control) and incubated to allow the formation of APP-Thr668Glu–JIP-1 complexes. Equal amounts of squid kinesin-1 were then added to the incubation mixtures. Putative complexes containing APP-Thr668Glu–JIP-1–kinesin-1 were immunoprecipitated and analyzed by immunoblotting. For immunoprecipitation,

we used an antibody to human APP that recognizes only ectopically expressed, phosphomimetic human APP and does not cross-react with the endogenous mouse APP; therefore, we immunoprecipitated only complexes containing phosphomimetic APP. Although binding of kinesin-1 to APP-Thr668Glu was low and variable in the absence of JIP-1, we consistently found increased amounts of kinesin-1 coprecipitating with APP-Thr668Glu from mixtures that contained JIP-1 (Fig. 4 A, top). Under the same experimental conditions that detected increased kinesin-1 recruitment to APP-Thr668Glu, we did not see any reproducible change in the amount of coprecipitated kinesin-1 when using lysates of CAD cells transfected with the nonphosphorylatable APP-Thr668Ala mutant (Fig. 4 A, bottom). These results suggest that JIP-1 preferentially facilitates recruitment of kinesin-1 to pAPP.

We also tested whether increased in vivo expression of JIP-1 in CAD cells resulted in enhanced transport of endogenous pAPP to neurite terminals. Owing to the dominant-negative effect of JIP-1 overexpression on JNK activity toward its substrates, high levels of JIP-1–FLAG decreased the overall production of pAPP (Muresan and Muresan, 2005) and prevented direct evaluation of the role of JIP-1 in the transport of pAPP. Therefore, we limited our analysis to those cells that expressed low levels of JIP-1–FLAG (see typical examples of such cells in Fig. 4, B–H). In these conditions, JIP-1–FLAG was largely localized to neurite terminals (Fig. 4, B–H), a distribution that closely resembled that of endogenous JIP-1 (see Fig. S5 A). Notably, the amount of pAPP that accumulated at the neurite endings was significantly increased (Fig. 4, B–H). We estimated that 80–90% of the CAD cells that expressed low levels of JIP-1–FLAG showed increased amounts of pAPP at neurite terminals compared with neighboring, nontransfected cells. This percentage dropped to <30% for cells transfected with myc-tagged Fe65, a protein that binds to APP at the same site as JIP-1. In addition, at neurite terminals, pAPP extensively colocalized with JIP-1–FLAG but not with Fe65-myc (colocalization coefficients 91 ± 5 vs. 23 ± 11; mean ± SD; Fig. 4, compare B–H with I–K). These results are consistent with increased transport of pAPP facilitated by the recruitment of kinesin-1 via JIP-1.

Fifth, conversely, we tested whether an increased amount of pAPP within cells led to increased transport of JIP-1. We transfected CAD cells with human APP-Thr668Glu that mimics pAPP and labeled it with the antibody 6E10 that preferentially recognizes human APP and not endogenous mouse APP (Fig. 4 L). Compared with the nontransfected cells (Fig. 4, L and M, short arrows), at moderate levels of expression of APP-Thr668Glu, endogenous JIP-1 appeared more efficiently accumulated at the tips of processes, and colocalized with APP-Thr668Glu (Fig. 4, L and M, long arrows). Overall, in >90% of transfected cells, we detected a strict correlation between the amount and distribution of exogenously expressed APP-Thr668Glu and JIP-1 at process terminals (Fig. 4, L–O and V [top]). No such correlation was seen in cells expressing low to moderate levels of wild-type APP (Fig. 4, S–U) or nonphosphorylatable APP-Thr668Ala mutant (Fig. 4, P–R and V, bottom). In addition, as shown in Fig. 4 (L and M), cells

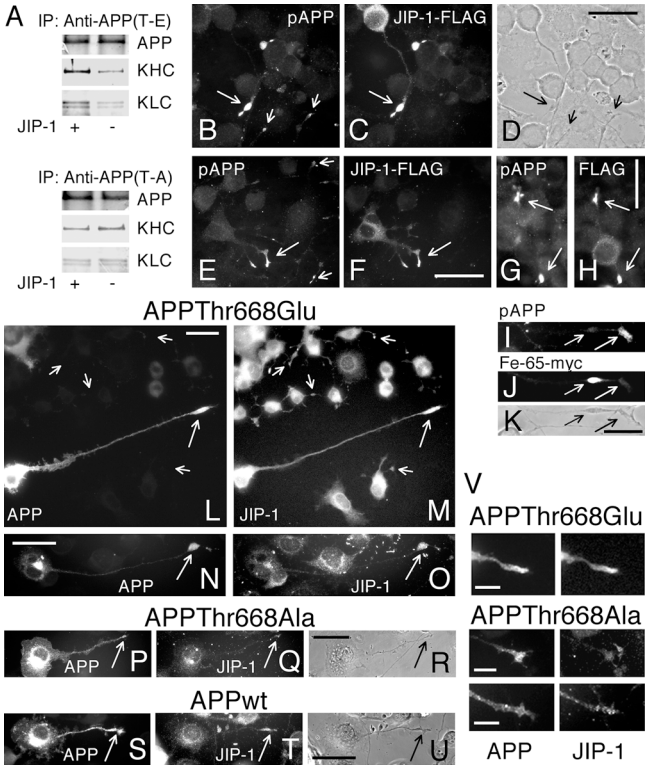

Figure 4. **JIP-1 facilitates the binding of kinesin-1 to pAPP and the transport of pAPP.** (A) Coprecipitation of kinesin-1 with constitutively phosphorylated, but not nonphosphorylatable APP, is enhanced by JIP-1. Lysates of CAD cells transfected with APP-Thr668Glu (APP(T-E)) or APP-Thr668Ala (APP(T-A)) were mixed with lysates of CAD cells transfected with JIP-1–FLAG (+) or of nontransfected (−) CAD cells. Squid kinesin-1 was added to the mixtures, and APP was immunoprecipitated with an antibody to human APP (mAbP2-1). Immunoprecipitated material was tested for the presence of KHC and KLC by immunoblotting. APP blots showed equal amounts of immunoprecipitated APP. Densitometric analysis of blots showed that, in the case of APP-Thr668Glu, approximately three times more kinesin-1 is coprecipitated from mixtures that contained JIP-1 (+). (B–K) CAD cells transfected with FLAG-tagged JIP-1 (B–H) or myc-tagged Fe65 (I–K) were double labeled for endogenous pAPP (B, E, G, and I) and the tag (C, F, H, and J). Note that the cells expressing JIP-1–FLAG show an increased amount of pAPP at the process terminals, which colocalizes with the expressed JIP-1 (B–H, long arrows). In contrast, pAPP does not colocalize with Fe65-myc (I–K). (B, E, and D) Short arrows point to the terminals of nontransfected cells. (L–V) Constitutively phosphorylated APP (APP-Thr668Glu), but not nonphosphorylatable APP (APP-Thr668Ala), promotes a more efficient transport of endogenous JIP-1 into CAD cell processes. Images show the localization of endogenous JIP-1 and exogenously expressed APP in CAD cells transfected with human wild-type APP (APPwt), APP-Thr668Ala, and APP-Thr668Glu. APP was detected with an antibody to the human protein that minimally cross-reacts with mouse APP (6E10). Note the increased presence of JIP-1 at the terminals of the cells transfected with APP-Thr668Glu (L–O, long arrows), but not APP–Thr668Ala (P–R, arrows). Short arrows in (L and M) point to the terminals of nontransfected cells. (V) Additional examples of immunolabeled neurite terminals of transfected cells, shown at high magnification. Bars: (B–H) and (L–U) 40 μm; (I–K) 20 μm; (V) 10 μm.

transfected with APP-Thr668Glu extended unusually long processes, a result that is consistent with a proposed role of pAPP in neurite extension (Ando et al., 1999; Muresan and Muresan, 2005). At high levels of expression, as predicted by our biochemical data (Fig. 2 C), all APP forms promoted increased JIP-1 transport, presumably a nonspecific result of overloading the system. Together, these data suggest that JIP-1

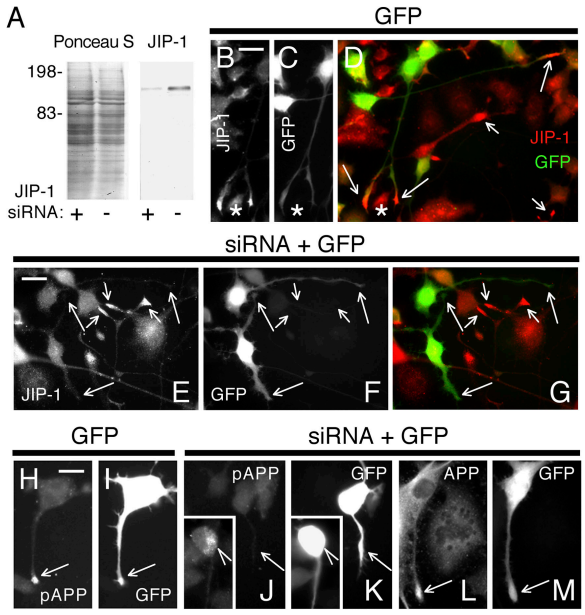

Figure 5. **JIP-1 is required for the accumulation of pAPP in neurites.** (A–G) Down-regulation of JIP-1 by siRNA. CAD cells were transfected with GFP cDNA with or without JIP-1–specific siRNA and analyzed by immunoblotting (A) and immunocytochemistry (B–G) for JIP-1 expression. Transfers of cell lysates were probed with anti–JIP-1 antibody, which detects one polypeptide in CAD cells (A). (A) Before blotting, transfers were stained with Ponceau S to compare protein loads. Molecular size markers are in kilodaltons. In immunofluorescence, cells transfected with GFP alone (control) accumulated JIP-1 at terminals (B–D; long arrows in D), similar to nontransfected cells (D, short arrows). No JIP-1 is detected at neurite endings (E–G, long arrows) in cells cotransfected with GFP and JIP-1–specific siRNA. (E–G) Short arrows point to terminals of nontransfected cells. Only the left portion of the image in D is shown in B and C. (B–D) The asterisks mark corresponding regions. (H–M) Down-regulation of JIP-1 leads to diminished accumulation of pAPP (J and K) but not total, mostly nonphosphorylated APP (L and M) in neurites. CAD cells were transfected with GFP alone (H and I; control) or with GFP and JIP-1–specific siRNA (J–M). Note that down-regulation of JIP-1 occasionally leads to accumulation of pAPP in the cell body (J and K, arrowheads in insets), likely because of impaired pAPP transport. pAPP localizes normally, at neurite endings, in cells transfected with GFP alone (H and I). Arrows point to process terminals. Bars, 20 μm.

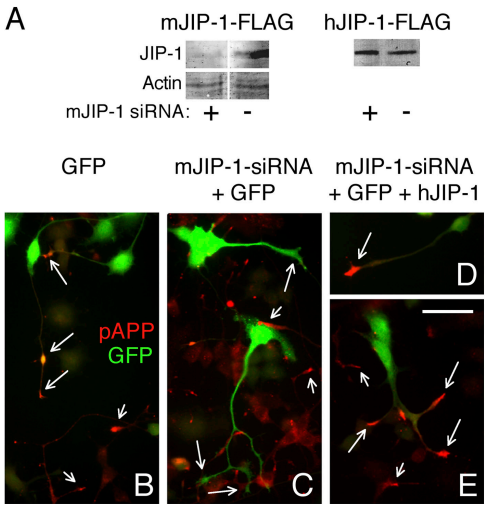

Figure 6. **Complementation of JIP-1–deficient CAD cells with human JIP-1 restores pAPP transport into neurites.** (A) Down-regulation of mouse JIP-1 (mJIP-1) but not human JIP-1 (hJIP-1) by mJIP-1–specific siRNA. CAD cells were transfected with FLAG-tagged mJIP-1 or hJIP-1 cDNA with or without mJIP-1–specific siRNA. Cell lysates were analyzed for expression of exogenous JIP-1 by immunoblotting with anti-FLAG antibody. The actin blot shows equal protein load. Note that mJIP-1–specific siRNA does not down-regulate hJIP-1 (right). (B–E) Rescue of pAPP transport by hJIP-1 in mJIP-1–deficient cells. CAD cells were transfected with GFP (B), GFP and mJIP-1–specific siRNA (C), or GFP, mJIP-1–specific siRNA, and hJIP-1–FLAG (D and E) and analyzed by immunocytochemistry for pAPP. Note that transfection with GFP alone does not affect localization of pAPP (B), whereas cotransfection with mJIP-1–specific siRNA eliminates accumulation of pAPP at neurite terminals (C). However, accumulation of pAPP at neurite endings is restored in cells transfected with hJIP-1 in addition to GFP and mJIP-1–specific siRNA (D and E). Long and short arrows point to the terminals of transfected and nontransfected cells, respectively. Bar, 50 μm.

and pAPP are cotransported by kinesin-1 as a complex. Phosphorylation of APP facilitates the formation and the transport of this complex, as well as an overall vesicular traffic that likely promotes the extension of neurites.

Finally, because increased availability of JIP-1 promoted transport of pAPP, we tested whether reduction in JIP-1 impairs transport of pAPP into neurites, i.e., whether JIP-1 is necessary for pAPP transport. We examined the distribution of pAPP in cells where JIP-1 expression was reduced by small interfering RNA (siRNA), a procedure that effectively decreased the level of endogenous JIP-1 (Fig. 5 A), as well as of JIP-1–FLAG when cotransfected in CAD cells (Fig. 6 A). For immunocytochemistry, JIP-1 siRNA was cotransfected with a GFP-encoding plasmid to allow the identification of JIP-1–depleted cells. Cells transfected with GFP alone, which were used as control, showed the typical accumulation of JIP-1 at terminals (Fig. 5, B–D). However, when cotransfected with JIP-1 siRNA, GFP was present in cells that had low levels of JIP-1 and lacked JIP-1 accumulation at neurite terminals (Fig. 5, E–G). With regard to pAPP, cells expressing GFP alone had normal, strong pAPP staining at the terminals, but only low staining in the cell body (Fig. 5, H and I). By contrast, CAD cells where JIP-1 expression was targeted by siRNA (Fig. 5, J and K) failed to accumulate pAPP at the terminals; instead, vesicles containing pAPP often accumulated in the cell body, suggesting a deficient transport of pAPP into neurites (Fig. 5, J and K, insets). This strong effect on transport was specific for pAPP because JIP-1 depletion did not alter the localization of total, mostly nonphosphorylated, APP in neurites (Fig. 5, L and M). Statistically, we found that <20% of siRNA-transfected cells that extended neurites contained pAPP at their terminals, a 4.5-fold reduction compared with untreated cells. This was similar to the fraction of siRNA-transfected cells that had detectable JIP-1 at terminals.

Transport of pAPP to neurite terminals in cells transfected with JIP-1 siRNA was restored by cotransfection of human JIP-1, a form that is not down-regulated by the mouse JIP-1 siRNA (Fig. 6). This result rules out the possibility that pAPP transport is indirectly suppressed in siRNA-transfected cells and confirms the role of JIP-1 in pAPP transport.

Accumulation of pAPP in the cell body upon treatment of cells with JIP-1 siRNA (see example in Fig. 5 [J and K, insets]) suggests that down-regulation of JIP-1 only affects the transport, but not the generation, of pAPP. We conclude that JIP-1 is required for the transport of pAPP into neurites, whereas the transport of nonphosphorylated APP appears independent of JIP-1.

JIP-2 can facilitate, but is not normally required for, accumulation of pAPP in neurites

These results indirectly suggest that JIP-2 (which also binds pAPP; Fig. 2 B) may play at best only a minor role in the transport of pAPP into neurites. We confirmed this hypothesis, using a similar experimental strategy based on immunolocalization of endogenous JIP-2 and pAPP, down-regulation of JIP-2 by siRNA, and overexpression of tagged JIP-2. Thus, in immunocytochemistry, JIP-2 showed an overall distribution pattern that differed from the distribution pattern of both JIP-1 and pAPP, particularly in the amount that entered the processes. Most JIP-2 was localized to the cell body and often only partially colocalized with JIP-1 and pAPP (Fig. S5, A–F, available at http://www.jcb.org/cgi/content/full/jcb.200502043/DC1). However, we did occasionally see a high degree of colocalization of JIP-2 with JIP-1 at neurite terminals (Fig. S5, A–C), but significantly less frequently than in the case of pAPP with JIP-1 (Fig. S5, G and H). Unlike for JIP-1, down-regulation of JIP-2 expression by siRNA (Fig. S5, I–L) did not prevent accumulation of pAPP at neurite endings (Fig. S5, M–O). However, as with JIP-1, the amount of pAPP accumulated at the neurite endings increased upon mild expression of JIP-2-FLAG (Fig. S5, P–R). We conclude that JIP-2 can facilitate transport of pAPP into CAD cell neurites, but it does not do so under normal conditions, when this function is largely performed by JIP-1.

Nonphosphorylated APP is transported into neuronal processes independent of pAPP

Together, the aforementioned results support a model where APP transport to neurites occurs via at least two pathways: a JIP-1–dependent route, responsible for the transport of the small fraction of cellular APP that is phosphorylated at Thr^{668}, and a JIP-1–independent pathway that carries over the nonphosphorylated APP, which represents the majority of cellular APP. This model implies that nonphosphorylated APP and pAPP should be associated with different vesicle populations. Indeed, immunocytochemistry of CAD cells shows a large fraction of APP in vesicles where pAPP was undetectable (Fig. 7, A–C). This segregation of nonphosphorylated APP from pAPP was also found in primary cultures of cortical neurons (Fig. 7 D), as well as in CAD cells that express APP-YFP (Fig. 7, E–H). Quantitatively, >80% of the total APP is present in vesicles lacking detectable pAPP. This result is not due to a failure of the antibodies to detect pAPP and nonphosphorylated APP simultaneously on the same vesicle because in cells transfected with APP-Thr668Glu, which is a mutant that is recognized by both the anti-APP and anti-pAPP antibodies, we found complete colocalization of pAPP and total APP (Fig. 7, I–K). This is certainly because of the fact that the phosphomimetic APP species is predominant. Thus, our results support the notion that pAPP and nonphosphorylated APP are largely segregated in separate transport vesicles.

Because the antibody to APP recognizes total (phosphorylated and nonphosphorylated) APP, we cannot exclude the possibility that some nonphosphorylated APP might be co-

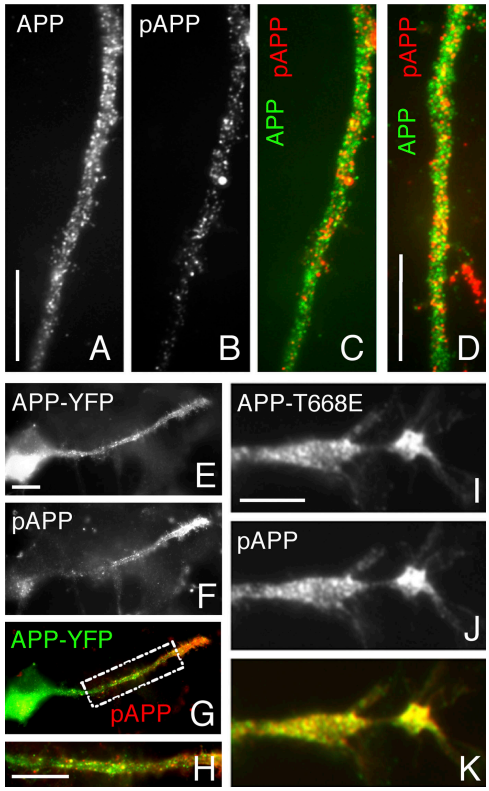

Figure 7. **Nonphosphorylated APP is largely segregated from pAPP during transport.** (A–D) Double labeling of endogenous, total APP (antibody 4G8; green) and pAPP (red) in CAD cells (A–C) and cortical neurons (D). Note that the antibody to total APP largely labels vesicles that do not stain for pAPP. The CAD cells shown in E–H and I–K have been transfected with APP-YFP (wild type) and nontagged APP-Thr668Glu (APP-T668E), respectively. Antibodies to total APP and pAPP label the same vesicle population in cells transfected with APP-Thr668Glu, where the constitutively phosphorylated APP predominates (I–K). This situation differs from the endogenous condition (nontransfected cells; A–D) or APP-YFP transfected cells (E–H), where only a fraction of APP is phosphorylated and sorted away from nonphosphorylated APP into distinct transport vesicles. Note that the antibody to pAPP cross-reacts with APP-Thr668Glu (I–K). H is an enlargement of the boxed area in G. Bars: (A–H) 10 μm; (I–K) 5 μm.

transported with pAPP. However, the majority of nonphosphorylated APP is localized to carrier vesicles that do not contain pAPP. We conclude that phosphorylated and nonphosphorylated APP are transported into neuronal processes by different pathways (both likely using kinesin-1) and that, under physiological conditions, JIP-1 mediates transport of pAPP, but not nonphosphorylated APP.

Discussion

APP and JIP-1 have been shown to be transported to neuronal terminals, where they might accomplish signaling functions, with possible implication in the pathobiology of Alzheimer's disease. To investigate their transport, we have studied the localization of endogenous JIP-1, total APP, and pAPP in CAD cells, and in primary cultures of hippocampal and cortical neurons, under conditions of normal differentiation, and under experimental circumstances aimed at interfering with recruitment to the cargo of kinesin-1. Because the localization of JIP-1,

total APP, and pAPP at neurite terminals is largely the result of active anterograde transport, this experimental approach allowed us to gain insight into the mechanism of this process. We found that in situ APP transport to terminals occurs via two separate populations of vesicles that—as detected by immunocytochemistry—differ in composition and whose transport is differentially regulated. Thus, ~80% of the APP-labeled vesicular structures along the neurites appear to carry only nonphosphorylated APP because they do not stain for pAPP; these vesicles also lack JIP-1. The transport of this vesicle population to the neurite terminal is independent of JIP-1. The remaining APP-containing vesicles (~20%) stain for pAPP and for JIP-1, and their transport to the terminal requires JIP-1. Taking into account the increased affinity of JIP-1 for pAPP over nonphosphorylated APP, these observations suggest that selective phosphorylation of a fraction of APP in the cell body triggers recruitment of JIP-1 to pAPP-containing vesicles, which then facilitates binding and/or activation of kinesin-1. The end result is the transport of pAPP–JIP-1–containing vesicles to the neurite terminals, which is where they accumulate. This process, unlike the seemingly constitutive transport of nonphosphorylated APP, appears to be the subject of at least two levels of regulation: the generation of pAPP and the recruitment of JIP-1. From a physiological point of view, these two levels of regulation would provide a stringent control for the availability of the putative pAPP–JIP-1 signaling complex at the neurite terminals.

Our immunocytochemical approach addresses the in situ situation, which is unaffected by protein overexpression. Because cells were fixed during a time of robust neurite extension, it is most likely that vesicles seen along the processes were engaged in anterograde transport. Indeed, we have shown that in CAD cells that express low levels of APP-YFP, >80% of the fluorescently labeled, motile vesicles moved anterogradely (Fig. S1) and, over extended periods of time, most of the fluorescently tagged vesicles were motile (>70%).

We found that JIP-1 is vesicle associated and colocalizes strictly with pAPP, but not with nonphosphorylated APP. It is intriguing that although JIP-1 is capable of binding to nonphosphorylated APP in vitro or when the two proteins are overexpressed in heterologous systems, endogenous JIP-1 apparently does not do so within neurites of cultured neurons in situ, where it colocalizes exclusively with pAPP. Our biochemical data confirm the ability of JIP-1 to interact with nonphosphorylated APP; however, we find that this binding is enhanced upon APP phosphorylation. Similarly, JIP-2 is capable of binding to pAPP in biochemical assays. Yet, it does not appear to play a major role in pAPP transport in vivo. The apparent discrepancy between the results obtained by in vitro biochemical assays and those from immunocytochemistry of endogenous proteins (where the interaction of JIP-1 to the nonphosphorylated APP is undetectable) might be accounted for by the complexity of the system in vivo. For example, in vivo JIP-1 might be prevented from binding to nonphosphorylated APP by other proteins (e.g., Fe65; Fig. 2 C) that may selectively bind to and block the JIP-1 binding site in nonphosphorylated APP. Technical advances will allow collection of data that accurately reflect the in vivo processes.

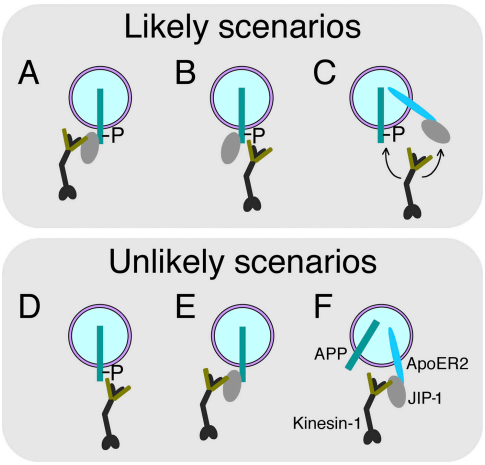

Figure 8. **Schematic representation of cotransport of JIP-1 and pAPP.** The diagram shows likely (i.e., experimentally supported; A–C) and unlikely (D–F) scenarios for transport of JIP-1, pAPP, and nonphosphorylated APP. (C) Kinesin-1 may bind to either pAPP or JIP-1. In vivo, pAPP is not transported without JIP-1 (D), and JIP-1 is not cotransported with nonphosphorylated APP (E and F).

Schematically, we created several likely (Fig. 8, A–C) and unlikely (Fig. 8, D–F) scenarios that fit our data regarding the interdependent transport of nonphosphorylated APP, pAPP, and JIP-1. The first two models (Fig. 8, A and B) emphasize the recruitment/activation of kinesin-1 by the pAPP–JIP-1 complex. The third model (Fig. 8 C), although in line with our results requiring the presence of JIP-1 on pAPP-containing vesicles, takes into account the possibility that the JIP-1–kinesin-1 complex might be recruited to other vesicle proteins, such as ApoER2 (Stockinger et al., 2000; Verhey et al., 2001). Consistent with our observation that down-regulation of JIP-1 blocks transport of pAPP into neurites, in all these models (Fig. 8, A–C) JIP-1 appears essential for the recruitment or activation of kinesin-1. The diagrams in Fig. 8 (D–F) represent situations that are not supported by our experimental results: transport of pAPP in the absence of JIP-1 (Fig. 8 D) and transport of nonphosphorylated APP with JIP-1 (Fig. 8, E and F).

In a separate study, we found that in differentiating CAD cells, APP is primarily phosphorylated by JNK, a kinase that binds to JIP-1 (Muresan and Muresan, 2005). Surprisingly, anchoring of JNK to APP via JIP-1—a potential mechanism for recruiting JNK to APP—does not appear to be required for APP phosphorylation because APP is still phosphorylated when JIP-1 expression is ablated by siRNA. Indeed, we recently reported that JIP-3, a JNK scaffolding protein unrelated to JIP-1, facilitates APP phosphorylation through a signaling pathway that specifically targets APP (Muresan and Muresan, 2005). Yet, JIP-1 seems to be essential for the transport of the already phosphorylated APP, as indicated by RNA interference experiments. Overall, our cumulative studies indicate that JIP-1 and JIP-3 are cotransported into neurites together with pAPP and accumulate as a complex at the growth cone. The coordinated action of these two JNK scaffolding proteins, resulting in APP phosphorylation and transport of the generated pAPP to the leading edge of extending neurites, is consistent with a

function of this large signaling complex in neurite growth (Ando et al., 1999; Muresan and Muresan, 2005). Further studies are required to elucidate the mechanisms by which APP, JIP-3, and JIP-1 may integrate JNK signaling with vesicular transport by kinesin-1 and neuronal differentiation.

Finally, our data suggest that a significant fraction of APP is transported to neurite terminals in a nonphosphorylated form, independently of pAPP and of JIP-1. Transport of nonphosphorylated APP may occur autonomously (i.e., constitutive) or in conjunction with other proteins that may bind to the cytoplasmic domain of APP, such as Fe65 or X11α/Mint-1 (i.e., regulated). Our data from experiments using a dominant-negative KLC domain that interferes with cargo binding are consistent with a role of kinesin-1 in the transport of nonphosphorylated APP as well. These results need to be cautiously interpreted because malfunction of kinesin-1 may indirectly impede the transport of APP, even if it was not the motor that carries the APP-containing vesicle. In the case of pAPP, however, our data argue strongly in favor of a JIP-1–facilitated recruitment of kinesin-1 to the cargo vesicle.

It is generally admitted that a deficient axonal transport may be one of the causes of Alzheimer's disease (Roy et al., 2005; Stokin et al., 2005). However, whether this may directly involve APP as a linker for kinesin-1, as previously proposed (Kamal et al., 2000), is currently highly debated, particularly because pull-down and coimmunoprecipitation experiments used to test the APP–kinesin-1 interaction are plagued by nonspecific binding (Matsuda et al., 2003; Lazarov et al., 2005). Moreover, the endogenous conditions are not faithfully reproduced after cell lysis or by overexpressing proteins that change the equilibrium between multiple, cross-interacting partners. We believe that the current debate will only be settled by addressing the transport of APP in experimental settings that are as close as possible to the endogenous conditions.

In conclusion, we found that transport of a fraction of APP by kinesin-1 occurs in concert with JIP-1, and this transport is regulated by the phosphorylation of APP. This implies that transport of JIP-1 is regulated by APP phosphorylation. Nonphosphorylated APP is transported on a different pathway, either through a direct interaction with the kinesin motor or by a yet to be identified mechanism. The two transport pathways appear to use distinct vesicle carriers and to be differently regulated. Further studies are required to fully understand the functional significance of pAPP–JIP-1 cotransport, likely relating these two proteins in a common signaling pathway.

Materials and methods

Antibodies

The following primary antibodies were used: mouse anti-Alzheimer precursor protein A4 (clone 22C11; CHEMICON International, Inc.); mouse anti–human amyloid-β protein (clones 4G8 and 6E10; Signet Laboratories); rabbit anti-APP (raised against a polypeptide from the cytoplasmic domain of APP; Cell Signaling Technology); mouse anti–human APP (mAbP2-1; BioSource International, Inc.); and mouse anti-KHC (clone H2; CHEMICON International, Inc.). The following anti–JIP-1 and anti–JIP-2 antibodies were used: goat (E-19) and mouse (B-7) anti–JIP-1; goat (C-20) and rabbit (H-95) anti–JIP-2 (all obtained from Santa Cruz Biotechnology, Inc.); and rabbit anti–JIP-1 (a gift from K. Verhey and B. Margolis, University of Michigan, Ann Arbor, MI; Meyer et al., 1999). A mouse antibody to KLC (63-90; Stenoien and Brady, 1997) was a gift from S. Brady (University of Illinois, Chicago, IL). A mouse antibody (K2.4) to kinesin-2 (detecting the 85-kD polypeptide corresponding to mammalian KIF3A; Cole et al., 1993) was a gift from J. Scholey (University of California, Davis, Davis, CA). A rabbit antibody to pAPP (BioSource International, Inc.) was raised against a phosphopeptide derived from the region surrounding Thr^{668} of human APP695, adsorbed against the nonphosphorylated peptide, and affinity purified with the antigen by the manufacturer. The antibody reacted with phosphorylated, but not with nonphosphorylated, forms of APP. Mouse antibodies to tags were used: anti–c-myc (Oncogene Research Products) and anti-FLAG (M2; Stratagene).

Cell cultures

The mouse central nervous system–derived catecholaminergic cell line CAD (obtained from D. Chikaraishi [Duke University Medical School, Durham, NC] and J. Wang [Cogent Neuroscience, Inc., Durham, NC]; Qi et al., 1997) was grown in 1:1 F12/DME medium, with 8% FBS and penicillin/streptomycin. CAD cell differentiation was induced by the removal of serum from the culture medium (Qi et al., 1997). Embrynic day 16.5 mouse cortical neurons (obtained from S. Cicero and K. Herrup, Case Western Reserve University, Cleveland, OH) were grown in neurobasal medium with B-27 supplement, L-glutamine, and penicillin/streptomycin for 5 d, with a change of media on day 4. Neurons were maintained in growth media until fixation for immunocytochemistry. COS-1 cells were grown in high-glucose DME, containing 10% FBS and penicillin/streptomycin. HEK293 cells were grown in RPMI 1640 containing 8% FBS.

Transfection

CAD, HEK293, and COS-1 cells were transfected according to the manufacturer's instructions, using either FuGene 6 (Roche Diagnostics) or Nucleofector technology (Amaxa Inc.). The HA-tagged KLC-TPR construct (containing all six TPRs) and the HA-PP5-TPR construct were previously described (Verhey et al., 2001). Constructs in pcDNA3 of human APP695 (wild-type and mutants [APP-Thr668Ala and APP-Thr668Glu]) were obtained from L.-H. Tsai (Harvard Medical School, Howard Hughes Medical Institute, Boston, MA). JIP constructs (pcMV-FLAG-JIP-1, pcDNA3-FLAG-JIP-2, and pcDNA3-FLAG-JIP-3) were obtained from R. Davis (University of Massachusetts Medical School, Howard Hughes Medical Institute, Worcester, MA; Whitmarsh et al., 1998; Yasuda et al., 1999; Kelkar et al., 2000). FLAG-tagged, human JIP-1e, and mouse JIP-1b constructs were obtained from L. D'Adamio (Albert Einstein College of Medicine, Bronx, NY; Scheinfeld et al., 2002). Myc-tagged Fe65 was obtained from B. Margolis (University of Michigan, Howard Hughes Medical Institute, Ann Arbor, MI; Borg et al., 1996). A pcDNA3/APP-YFP (human APP695) construct was obtained from C. Dotti (Cavalieri Ottolenghi Scientific Institute, Università degli Studi di Torino, Torino, Italy) and C. Kaether (European Molecular Biology Laboratory, Heidelberg, Germany; Kaether et al., 2000).

RNA interference experiments

For immunocytochemistry, CAD cells were cotransfected with pmaxGFP (Amaxa Inc.) and either mouse JIP-1–specific (Santa Cruz Biotechnology, Inc.) or JIP-2–specific (Ambion) siRNA. In JIP-1 complementation experiments, cells were cotransfected with pmaxGFP, human JIP-1, and mouse JIP-1–specific siRNA. Cells were allowed to attach to the coverslip in the presence of serum and cultured for 24–48 h in the absence of serum. For biochemistry experiments, cells were transfected with either pmaxGFP or FLAG-tagged JIP-1 (mouse or human) in the presence or absence of JIP-1–specific siRNA. After differentiation, cells were collected in sample buffer and analyzed by Western blotting for expressed proteins.

Pull-down and coimmunoprecipitation experiments

COS-1 cells transfected with cDNAs encoding FLAG-tagged JIPs were rinsed with phosphate-buffered saline and extracted after 30 min at 4°C in lysis buffer (10 mM Tris-HCl, pH 7.5, 50 mM NaCl, 4 mM EDTA, and 1% NP-40) containing leupeptin, pepstatin, aprotinin (10 μg/ml each), 5 mM benzamidin, 1 mM PMSF, and phosphatase inhibitors (1 mM Na vanadate, 5 mM NaF, and 25 mM β-glycerophosphate). Extracts were centrifuged for 10 min at 16,000 *g* and incubated 12–16 h at 4°C with NH_2-terminally biotinylated polypeptides corresponding to the entire cytoplasmic domain of APP (starting with lysine) that were chemically synthesized with either phosphorylated or nonphosphorylated Thr (corresponding to Thr^{668} in APP695). Protein complexes containing the polypeptides were collected on streptavidin-Sepharose and analyzed by SDS-PAGE and immunoblotting (Muresan et al., 2000) with anti-tag antibodies. Polypeptides corresponding to the APP cytoplasmic domain were separated in 16.5% Tris-tricine gels (Bio-Rad Laboratories).

In immunoprecipitation experiments that tested the role of JIP-1 in the recruitment of kinesin-1 to APP, CAD cells were separately transfected with human APP-Thr668Glu (or APP–Thr668Ala) and JIP-1–FLAG. Extracts of APP-transfected cells were mixed with extracts from JIP-1–transfected or nontransfected cells and incubated for 2 h at 4°C with a purified fraction of squid kinesin-1 (Muresan et al., 1996). APP was immunoprecipitated from the incubation mixtures with the antibody mAbP2-1 overnight at 4°C. In experiments that tested the interaction of JIP-1 with APP and pAPP, CAD cells were separately transfected with human APP695 and JIP-1–FLAG. Cell extracts were mixed and incubated overnight in the presence of phosphatase inhibitors. JIP-1 and associated proteins were immunoprecipitated from the mixture with anti-FLAG antibody. In control experiments, JIP-1–FLAG–containing cytosol was replaced with cytosol from nontransfected cells. In all cases, the collection of immunoprecipitated material on protein A–Sepharose-4B and extraction of the beads in SDS-PAGE sample buffer was done as previously described (Muresan and Arvan, 1997). Immunoprecipitated material was analyzed by Western blotting. Image software (National Institutes of Health) was used for densitometric analysis of immunoblots. In all immunoprecipitation experiments, extracts that contained low levels of JIP-1–FLAG were used.

ELISA

Biotinylated APP polypeptides (with phosphorylated or nonphosphorylated Thr^{668}) were adsorbed to Reacti-Bind NeutrAvidin-coated Plates that were preblocked with SuperBlock Blocking Buffer (Pierce Chemical Co.). Cytosolic fractions containing increasing levels of JIP-1–FLAG or Fe65-myc were prepared by mixing decreasing volumes of cytosol from nontransfected HEK293 cells with increasing volumes of cytosol from transfected cells. Cytosol concentration was thus kept constant throughout the assay. The plates were incubated with these fractions, then with alkaline phosphatase–conjugated antibodies to FLAG or myc, and processed for colorimetric reaction, followed by an OD reading at 405 nm, according to the manufacturer's protocol.

Preparation of brain extracts

Brain tissue was collected from neonatal (P2) or 5-week-old male Sprague-Dawley rats (killed by asphyxiation with CO_2; protocol approved by the Institutional Animal Care and Use Committee at Case Western Reserve University), placed in ice-cold phosphate-buffered saline, pH 7.4, and homogenized in Hepes–acetate buffer (50 mM K-Hepes, 50 mM K-acetate, 5 mM EGTA, 5 mM Mg acetate, 1 mM Na vanadate, 5 mM NaF, and 25 mM β-glycerophosphate, pH 7.4) containing protease inhibitors. Extracts were analyzed for the presence of JIP-1, APP, and pAPP by Western blotting. Incubations with anti-pAPP antibodies were done in the presence or absence of competitor polypeptides (i.e., biotinylated, phosphorylated, or nonphosphorylated polypeptides that encompassed the entire APP cytoplasmic domain) at 100:1 molar excess over IgG.

Immunocytochemistry

Transfected or nontransfected CAD cells and primary cultures of cortical neurons were fixed for 20 min in phosphate-buffered saline containing 4% formaldehyde and 4% sucrose, permeabilized with 0.3% Triton X-100 for 20 min at 20°C, and processed for single or double antigen labeling as previously described (Muresan et al., 1998). Secondary antibodies (goat anti–mouse/rabbit IgG or donkey anti–goat/mouse/rabbit IgG) coupled to Alexa dyes (Alexa Fluor 488 and Alexa Fluor 594) were obtained from Invitrogen. When required, double labeling experiments with two primary antibodies raised in rabbit were done using fluorescently labeled, monovalent Fab fragments of anti–rabbit IgG (Jackson ImmunoResearch Laboratories; Li et al., 2002). In control experiments, immunolabeling with anti-pAPP antibody was done in the presence of phosphorylated or nonphosphorylated polypeptides (100:1 molar excess over IgG) that encompassed either a 12–amino acid region centered on Thr^{668} or the entire APP cytoplasmic domain. Transfected human APP was selectively detected with antibody 6E10 that does not detect endogenous mouse APP. Unless otherwise specified, endogenous JIP-1 and total APP were detected with goat polyclonal and mouse monoclonal (4G8) antibodies, respectively. Digital images were obtained with two different microscopes (Model Axiophot; Carl Zeiss MicroImaging, Inc.; or model Optiphot; Nikon; 100× oil, 20×, and 40× objectives) equipped with cooled charge-coupled device cameras (Olympus) and collected using either Openlab (Improvision Inc.) or Magnafire (Optronics) image analysis software. Images were processed for contrast and brightness using Photoshop software (Adobe). In some cases, samples were analyzed by confocal microscopy; in others, images were collected on a microscope (DeltaVision RT) and subjected to deconvolution analysis.

In vivo motility

Motility of APP-YFP–containing vesicles was visualized in vivo, in thin processes of transiently transfected CAD cells. The experimental set-up consisted of an inverted microscope (model TE200U; Nikon), a camera (model CoolSnapHQ; Roper), and MetaMorph software (Molecular Devices). Kymographs (Silverman et al., 2001) were generated from successive images acquired at 0.502 frames/s and used for quantifying anterograde and retrograde motile and stationary vesicles.

Quantitative analysis

The degree of colocalization of various antigen pairs was quantified as follows. First, the mean pixel intensity for each pair of images was determined in Photoshop 7.0 (Adobe; Sabo et al., 2003). Second, images were thresholded at the mean intensity, to eliminate most of the diffuse, nonparticulate labeling. Finally, the thresholded images were multiplied. The resulting image showed nonzero pixel intensities only in regions of colocalization, i.e., regions were pixel intensity differed from zero in both images. Percentages of colocalization were calculated by dividing the number of pixels of nonzero intensities in the product image by the number of pixels of nonzero intensities in the parental images.

In experiments that probed pAPP localization in cells transfected with JIP-1–FLAG or Fe65-myc, coefficients of colocalization of pAPP with the tagged proteins were obtained using Image-Pro Plus software (Media Cybernetics, Inc.; Manders et al., 1993). The percentage of transfected cells that showed increased pAPP at neurite terminals was estimated by comparison with nontransfected cells present in the microscopic field. For each experiment, 20–30 microscopic fields, each containing at least one transfected cell expressing the tagged protein at a low level, were analyzed. Cells were judged as expressing low levels of JIP-1–FLAG if cell bodies contained little tagged protein compared with the processes. Experiments with JIP-1–FLAG–transfected cells were done in duplicate.

Online supplemental material

Fig. S1 shows that most of the fluorescently labeled vesicles move anterogradely within neurites of CAD cells transfected with APP-YFP. Fig. S2 characterizes by Western blotting and immunocytochemistry the main antibodies used in this study and shows specificity of the anti-pAPP antibody strictly for pAPP. Fig. S3 shows colocalization of pAPP with microtubules and kinesin-1, but not kinesin-2, in CAD cell processes. Fig. S4 shows that localization of total APP to neurites is kinesin-1 dependent. Fig. S5 shows that JIP-2 is not required for the accumulation of pAPP in neurites. Online supplemental material is available at http://www.jcb.org/cgi/content/full/jcb.200502043/DC1.

We thank Drs. Dona Chikaraishi and James Wang for kindly providing the CAD cell line; Samantha Cicero and Dr. Karl Herrup for kindly providing the cortical neuron cultures; Drs. Li-Huei Tsai and Ming-Sum Lee for kindly providing cDNA constructs and an antibody to phosphorylated APP that was used in preliminary experiments; and Drs. Luciano D'Adamio, Scott Brady, Roger Davis, Carlos Dotti, Christoph Kaether, Ben Margolis, and Jonathan Scholey for kindly providing cDNA constructs and antibodies.

This work was supported by National Institutes of Health grant 5R01GM068596-02, a Mount Sinai Health Care Foundation Scholarship, and Pilot grant AG08012 from the Alzheimer's Disease Research Center at the University Hospitals of Cleveland and Case Western Reserve University (V. Muresan).

Submitted: 7 February 2005
Accepted: 17 October 2005

References

Ando, K., M. Oishi, S. Takeda, K. Iijima, T. Isohara, A.C. Nairn, Y. Kirino, P. Greengard, and T. Suzuki. 1999. Role of phosphorylation of Alzheimer's amyloid precursor protein during neuronal differentiation. *J. Neurosci.* 19:4421–4427.

Ando, K., K.I. Iijima, J.I. Elliott, Y. Kirino, and T. Suzuki. 2001. Phosphorylation-dependent regulation of the interaction of amyloid precursor protein with Fe65 affects the production of beta-amyloid. *J. Biol. Chem.* 276:40353–40361.

Borg, J.P., J. Ooi, E. Levy, and B. Margolis. 1996. The phosphotyrosine interaction domains of X11 and FE65 bind to distinct sites on the YENPTY motif of amyloid precursor protein. *Mol. Cell. Biol.* 16:6229–6241.

Cole, D.G., S.W. Chinn, K.P. Wedaman, K. Hall, T. Vuong, and J.M. Scholey. 1993. Novel heterotrimeric kinesin-related protein purified from sea urchin eggs. *Nature.* 366:268–270.

Iijima, K., K. Ando, S. Takeda, Y. Satoh, T. Seki, S. Itohara, P. Greengard, Y. Kirino, A.C. Nairn, and T. Suzuki. 2000. Neuron-specific phosphorylation of Alzheimer's beta-amyloid precursor protein by cyclin-dependent kinase 5. *J. Neurochem.* 75:1085–1091.

Inomata, H., Y. Nakamura, A. Hayakawa, H. Takata, T. Suzuki, K. Miyazawa, and N. Kitamura. 2003. A scaffold protein JIP-1b enhances amyloid precursor protein phosphorylation by JNK and its association with kinesin light chain 1. *J. Biol. Chem.* 278:22946–22955.

Kaether, C., P. Skehel, and C.G. Dotti. 2000. Axonal membrane proteins are transported in distinct carriers: a two-color video microscopy study in cultured hippocampal neurons. *Mol. Biol. Cell.* 11:1213–1224.

Kamal, A., G.B. Stokin, Z. Yang, C. Xia, and L.S. Goldstein. 2000. Axonal transport of amyloid precursor protein is mediated by direct binding to the kinesin light chain subunit of kinesin-I. *Neuron.* 28:449–459.

Kelkar, N., S. Gupta, M. Dickens, and R.J. Davis. 2000. Interaction of a mitogen-activated protein kinase signaling module with the neuronal protein JIP3. *Mol. Cell. Biol.* 20:1030–1043.

Lazarov, O., G.A. Morfini, E.B. Lee, M.H. Farah, A. Szodorai, S.R. DeBoer, V.E. Koliatsos, S. Kins, V.M. Lee, P.C. Wong, et al. 2005. Axonal transport, amyloid precursor protein, kinesin-1, and the processing apparatus: revisited. *J. Neurosci.* 25:2386–2395.

Lee, E.B., B. Zhang, K. Liu, E.A. Greenbaum, R.W. Doms, J.Q. Trojanowski, and V.M. Lee. 2005. BACE overexpression alters the subcellular processing of APP and inhibits Aβ deposition in vivo. *J. Cell Biol.* 168:291–302.

Lee, M.S., S.C. Kao, C.A. Lemere, W. Xia, H.C. Tseng, Y. Zhou, R. Neve, M.K. Ahlijanian, and L.H. Tsai. 2003. APP processing is regulated by cytoplasmic phosphorylation. *J. Cell Biol.* 163:83–95.

Li, X., S.H. Low, M. Miura, and T. Weimbs. 2002. SNARE expression and localization in renal epithelial cells suggest mechanism for variability of trafficking phenotypes. *Am. J. Physiol. Renal Physiol.* 283:F1111–F1122.

Manders, E.M.M., F.J. Verbeek, and J.A. Aten. 1993. Measurement of co-localization of objects in dual-colour confocal images. *J. Microsc.* 169:375–382.

Matsuda, S., T. Yasukawa, Y. Homma, Y. Ito, T. Niikura, T. Hiraki, S. Hirai, S. Ohno, Y. Kita, M. Kawasumi, et al. 2001. c-Jun N-terminal kinase (JNK)-interacting protein-1b/islet-brain-1 scaffolds Alzheimer's amyloid precursor protein with JNK. *J. Neurosci.* 21:6597–6607.

Matsuda, S., Y. Matsuda, and L. D'Adamio. 2003. Amyloid beta protein precursor (AbetaPP), but not AbetaPP-like protein 2, is bridged to the kinesin light chain by the scaffold protein JNK-interacting protein 1. *J. Biol. Chem.* 278:38601–38606.

Meyer, D., A. Liu, and B. Margolis. 1999. Interaction of c-Jun amino-terminal kinase interacting protein-1 with p190 rhoGEF and its localization in differentiated neurons. *J. Biol. Chem.* 274:35113–35118.

Muresan, V. 2000. One axon, many kinesins: what's the logic? *J. Neurocytol.* 29:799–818.

Muresan, V., C.P. Godek, T.S. Reese, and B.J. Schnapp. 1996. Plus-end motors override minus-end motors during transport of squid axon vesicles on microtubules. *J. Cell Biol.* 135:383–397.

Muresan, V., T. Abramson, A. Lyass, D. Winter, E. Porro, F. Hong, N.L. Chamberlin, and B.J. Schnapp. 1998. KIF3C and KIF3A form a novel neuronal heteromeric kinesin that associates with membrane vesicles. *Mol. Biol. Cell.* 9:637–652.

Muresan, Z., and P. Arvan. 1997. Thyroglobulin transport along the secretory pathway. Investigation of the role of molecular chaperone, GRP94, in protein export from the endoplasmic reticulum. *J. Biol. Chem.* 272:26095–26102 (published erratum appears in *J. Biol. Chem.* 1997. 272:30590)

Muresan, Z., and V. Muresan. 2004. A phosphorylated, carboxy-terminal fragment of {beta}-amyloid precursor protein localizes to the splicing factor compartment. *Hum. Mol. Genet.* 13:475–488.

Muresan, Z., and V. Muresan. 2005. c-Jun NH2-terminal kinase-interacting protein-3 facilitates phosphorylation and controls localization of amyloid-beta precursor protein. *J. Neurosci.* 25:3741–3751.

Muresan, Z., D.L. Paul, and D.A. Goodenough. 2000. Occludin 1B, a variant of the tight junction protein occludin. *Mol. Biol. Cell.* 11:627–634.

Pigino, G., G. Morfini, A. Pelsman, M.P. Mattson, S.T. Brady, and J. Busciglio. 2003. Alzheimer's presenilin 1 mutations impair kinesin-based axonal transport. *J. Neurosci.* 23:4499–4508.

Qi, Y., J.K. Wang, M. McMillian, and D.M. Chikaraishi. 1997. Characterization of a CNS cell line, CAD, in which morphological differentiation is initiated by serum deprivation. *J. Neurosci.* 17:1217–1225.

Roy, S., B. Zhang, V.M. Lee, and J.Q. Trojanowski. 2005. Axonal transport defects: a common theme in neurodegenerative diseases. *Acta Neuropathol. (Berl.).* 109:5–13.

Sabo, S.L., A.F. Ikin, J.D. Buxbaum, and P. Greengard. 2003. The amyloid precursor protein and its regulatory protein, FE65, in growth cones and synapses in vitro and in vivo. *J. Neurosci.* 23:5407–5415.

Scheinfeld, M.H., R. Roncarati, P. Vito, P.A. Lopez, M. Abdallah, and L. D'Adamio. 2002. Jun NH2-terminal kinase (JNK) interacting protein 1 (JIP1) binds the cytoplasmic domain of the Alzheimer's beta-amyloid precursor protein (APP). *J. Biol. Chem.* 277:3767–3775.

Selkoe, D.J. 1998. The cell biology of beta-amyloid precursor protein and presenilin in Alzheimer's disease. *Trends Cell Biol.* 8:447–453.

Silverman, M.A., S. Kaech, M. Jareb, M.A. Burack, L. Vogt, P. Sonderegger, and G. Banker. 2001. Sorting and directed transport of membrane proteins during development of hippocampal neurons in culture. *Proc. Natl. Acad. Sci. USA.* 98:7051–7057.

Stamer, K., R. Vogel, E. Thies, E. Mandelkow, and E.M. Mandelkow. 2002. Tau blocks traffic of organelles, neurofilaments, and APP vesicles in neurons and enhances oxidative stress. *J. Cell Biol.* 156:1051–1063.

Stenoien, D.L., and S.T. Brady. 1997. Immunochemical analysis of kinesin light chain function. *Mol. Biol. Cell.* 8:675–689.

Stockinger, W., C. Brandes, D. Fasching, M. Hermann, M. Gotthardt, J. Herz, W.J. Schneider, and J. Nimpf. 2000. The reelin receptor ApoER2 recruits JNK-interacting proteins-1 and -2. *J. Biol. Chem.* 275:25625–25632.

Stokin, G.B., C. Lillo, T.L. Falzone, R.G. Brusch, E. Rockenstein, S.L. Mount, R. Raman, P. Davies, E. Masliah, D.S. Williams, and L.S. Goldstein. 2005. Axonopathy and transport deficits early in the pathogenesis of Alzheimer's disease. *Science.* 307:1282–1288.

Taru, H., K. Iijima, M. Hase, Y. Kirino, Y. Yagi, and T. Suzuki. 2002. Interaction of Alzheimer's beta-amyloid precursor family proteins with scaffold proteins of the JNK signaling cascade. *J. Biol. Chem.* 277:20070–20078.

Verhey, K.J., D. Meyer, R. Deehan, J. Blenis, B.J. Schnapp, T.A. Rapoport, and B. Margolis. 2001. Cargo of kinesin identified as JIP scaffolding proteins and associated signaling molecules. *J. Cell Biol.* 152:959–970.

Wasco, W., S. Gurubhagavatula, M.D. Paradis, D.M. Romano, S.S. Sisodia, B.T. Hyman, R.L. Neve, and R.E. Tanzi. 1993. Isolation and characterization of APLP2 encoding a homologue of the Alzheimer's associated amyloid beta protein precursor. *Nat. Genet.* 5:95–100.

Whitmarsh, A.J., J. Cavanagh, C. Tournier, J. Yasuda, and R.J. Davis. 1998. A mammalian scaffold complex that selectively mediates MAP kinase activation. *Science.* 281:1671–1674.

Whitmarsh, A.J., C.Y. Kuan, N.J. Kennedy, N. Kelkar, T.F. Haydar, J.P. Mordes, M. Appel, A.A. Rossini, S.N. Jones, R.A. Flavell, et al. 2001. Requirement of the JIP1 scaffold protein for stress-induced JNK activation. *Genes Dev.* 15:2421–2432.

Yamazaki, T., D.J. Selkoe, and E.H. Koo. 1995. Trafficking of cell surface beta-amyloid precursor protein: retrograde and transcytotic transport in cultured neurons. *J. Cell Biol.* 129:431–442.

Yasuda, J., A.J. Whitmarsh, J. Cavanagh, M. Sharma, and R.J. Davis. 1999. The JIP group of mitogen-activated protein kinase scaffold proteins. *Mol. Cell. Biol.* 19:7245–7254.